Published in final edited form as:
Neuropharmacology. 2009 ; 56(6-7): 1017–1026. doi:10.1016/j.neuropharm.2009.02.005.

Persistent Inflammatory Pain Decreases the Antinociceptive Effects of the *Mu* Opioid Receptor Agonist DAMGO in the Locus Coeruleus of Male Rats

Amy C. Jongeling[b,c], **Malcolm E. Johns**[d], **Anne Z. Murphy**[d], and **Donna L. Hammond**[a,b]

a *Department of Anesthesia, The University of Iowa, Iowa City, IA 52242*

b *Graduate Program in Neuroscience, The University of Iowa, Iowa City, IA 52242*

c *Medical Scientist Training Program, The University of Iowa, Iowa City, IA 52242*

d *Neuroscience Institute, Center for Behavioral Neurosciences Georgia State University, Atlanta, GA 30302*

Abstract

Persistent inflammatory nociception increases levels of endogenous opioids with affinity for *delta* opioid receptors in the ventromedial medulla and enhances the antinociceptive effects of the *mu* opioid receptor (MOPr) agonist [D-Ala^2-NMePhe^4, Gly^5-ol]enkephalin (DAMGO) (Hurley and Hammond, 2001). It also increases levels of endogenous opioids that act at MOPr elsewhere in the CNS (Zangen et al., 1998). This study tested the hypothesis that a sustained release of endogenous opioids leads to a downregulation of MOPr in the locus coeruleus (LC) and induces a state of endogenous opioid tolerance. Four days after injection of complete Freund's adjuvant (CFA) in the left hindpaw of the rat, both the magnitude and duration of the antinociception produced by microinjection of DAMGO in the right LC were reduced. Saturation isotherms demonstrated a 50% decrease in MOPr B_{max} in homogenates of the LC from CFA-treated rats; K_d was unchanged. Receptor autoradiography revealed that this decrease was bilateral. The decreased efficacy of DAMGO in CFA-treated rats most likely results from a decreased number of MOPr in the LC. Microinjection of the MOPr antagonist D-Phe-Cys-Tyr-D-Trp-Arg-Thr-Pen-Thr-NH_2 (CTAP) in the LC did not exacerbate hyperalgesia in the ipsilateral hindpaw or produce hyperalgesia in the contralateral hindpaw of CFA-treated rats. The downregulation in MOPr is therefore unlikely to result from the induction of endogenous opioid tolerance in the LC. These results indicate that persistent inflammatory nociception alters the antinociceptive actions of MOPr agonists in the CNS by diverse mechanisms that are nucleus specific and likely to have different physiological implications.

Keywords

anti-hyperalgesia; antinociception; complete Freund's adjuvant; mu opioid receptor; DAMGO; CTAP

Correspondence to: Donna L. Hammond, Ph.D. Department of Anesthesia, The University of Iowa, 200 Hawkins Drive 6 JCP, Iowa City, IA 52242, +1-319-384-7127 (voice), +1-319-356-2940 (fax), E-mail: donna-hammond@uiowa.edu.

1. Introduction

The locus coeruleus (LC) plays an important role in the modulation of nociception (Millan, 2002; Pertovaara, 2006). Noxious stimuli activate neurons in the LC bilaterally (Clement et al., 1996; Hirata and Aston-Jones, 1994), induce expression of Fos protein in LC neurons bilaterally (Tsuruoka et al., 2003) and increase the release of norepinephrine in the spinal cord (Tsuruoka et al., 1999). Ablation of the LC exacerbates thermal hyperalgesia (Tsuruoka and Willis, 1996) and enhances the expression of Fos protein by dorsal horn neurons in response to a noxious stimulus in acute and subacute inflammatory pain states (Wei et al., 1999). As electrical or chemical activation of LC neurons produces antinociception (Pertovaara, 2006), the latter findings suggest that inflammatory injury causes a compensatory activation of LC neurons that functions to diminish the magnitude of inflammatory hyperalgesia.

The rostral ventromedial medulla (RVM) is also implicated in the modulation of nociception and the production of antinociception by opioids (Millan, 2002). Under conditions of persistent inflammatory nociception, the anti-hyperalgesic and antinociceptive effects of *mu* opioid receptor (MOPr) agonists microinjected in the RVM are enhanced (Hurley and Hammond, 2000; Schepers et al., 2007). The mechanism does not appear to entail an increase in receptor number, affinity or G-protein activation, but rather a synergistic or additive interaction of the exogenously applied MOPr agonist with increased levels of endogenous opioid peptides in the RVM that have preferential affinity for *delta* opioid receptors (Hurley and Hammond, 2001; Sykes et al., 2007).

Persistent inflammatory nociception also increases the release of endogenous opioids elsewhere in the CNS. For example, levels of β-endorphin are increased in the periaqueductal gray and arcuate nucleus after the induction of inflammatory nociception (Porro et al., 1991; Zangen et al., 1998). The LC has a very high density of MOPr (Ding et al., 1996; Mansour et al., 1994), and is innervated by fibers that are immunoreactive for endogenous opioid peptides that act at MOPr (Peoples et al., 2002; Van Bockstaele et al., 1995). However, it is not known how persistent inflammatory nociception affects the release of endogenous opioid peptides or MOPr function in the LC. Whole-cell voltage clamp recordings indicate that the postsynaptic effects of a MOPr agonist are diminished in LC neurons from rats with persistent inflammatory nociception induced by injection of complete Freund's adjuvant (CFA) in the hindpaw (Jongeling et al., 2005). This finding led us to propose that chronic inflammatory nociception causes a sustained release of endogenous opioid peptides in the LC leading to a desensitization or downregulation of MOPr in LC neurons that then induces a state of endogenous opioid tolerance. Three predictions that arise from this hypothesis are (1) the antinociceptive effects of a MOPr agonist microinjected in the LC are decreased in CFA-treated rats; (2) antagonism of endogenously released opioids that act at MOPr in the LC exacerbates thermal hyperalgesia in the inflamed hindpaw and induces thermal hyperalgesia in the contralateral hindpaw of CFA-treated rats' and (3) the number or affinity of MOPr in the LC is decreased in CFA-treated rats. The results support our prediction that persistent inflammatory pain reduces the antinociceptive efficacy of MOPr agonists in the LC, most likely by reducing the number of MOPr in the LC. However, the findings do not support the induction of a state of endogenous tolerance at MOPr resulting from a sustained release of endogenous opioids in the LC. These results provide new evidence that persistent inflammatory nociception alters the antinociceptive actions of MOPr agonists in the CNS by diverse mechanisms that are specific to the nucleus and likely to have different physiological implications.

2. Methods

This study comprised the behavioral and neurochemical correlate of an *in vitro* electrophysiological investigation of the actions of MOPr agonists on LC neurons in brainstem

slices (Jongeling et al., 2005). The viability and visibility of neurons in brainstem slices decrease significantly with age, factors that introduce significant technical challenges to whole-cell patch-clamp recordings. These issues were circumvented by using young rats 24 to 29 days of age. For consistency, the behavioral experiments were conducted in male Sprague Dawley rats of the same age (Harlan; Indianapolis, IN). All litters were weaned at 21 days old; testing began at 24 or 25 days of age. These experiments were approved by the University of Iowa Animal Care and Use Committee, and were conduced in accordance with the guidelines of the National Institutes of Health Guide for the Care and Use of Laboratory Animals and the guidelines of the International Association for the Study of Pain. Every effort was made to minimize the number of rats used and their suffering.

2.1. Assessment of Nociceptive Threshold

Nociceptive threshold was assessed by paw withdrawal latency (PWL) to radiant heat (Hurley and Hammond, 2000). Rats were acclimated to the testing environment for 30 min, and then allowed to move freely for another 15 min within a small Plexiglas® enclosure resting on an elevated glass plate that was maintained at 25°C (UARD group, LaJolla CA). A beam of light was then positioned under each hindpaw while it was resting flat on the glass plate, and latency to withdrawal of the hindpaw from the thermal stimulus was recorded. If the rat did not withdraw its paw within 20 s, the test was terminated to prevent tissue injury and the rat was assigned this value. Only rats that responded to the stimulus with baseline PWL ranging between 7.5 and 12 s at the outset of the study were used.

2.2. Implantation of Intracerebral Guide Cannulae

After determination of baseline PWL, rats were anesthetized with a mixture of ketamine hydrochloride (70 mg/kg i.p.) and xylazine (9 mg/kg i.p.) and placed in a stereotaxic apparatus. An intracerebral guide cannula (26 gauge; Plastics One Inc., Roanoke, VA) was implanted into the right LC (8.8 mm caudal from bregma, 1.5 mm right of midline) such that it terminated 2 mm dorsal to the LC. A 33-gauge stainless steel wire obdurator was placed in the guide cannula to maintain patency. Care was taken to ensure that the skull was perfectly dry before the cannula was secured to it with a combination of cyanoacrylate and dental acrylic. Also, the skin edges were not sutured, but allowed to naturally retract against the base of the pedestal. After surgery, rats were housed no more than five per cage on a 12-h light/dark cycle with free access to food and water. Special care was taken to keep the pedestal clean. Thus, there was little in the way of an attractive nuisance for cagemates and > 98% of rats maintained their cannulae over the four day recovery period

2.3 Microinjection Procedure, Histology and Drugs

The MOPr agonist [D-Ala^2, N-Me-Phe^4, Gly^5-ol]enkephalin (DAMGO) and the MOPr antagonist D-Phe-Cys-Tyr-D-Trp-Arg-Thr-Pen-Thr-NH_2 (CTAP) were obtained from Sigma-Aldrich (St. Louis, MO). Both drugs were dissolved in pH 7.4 saline. All drugs or drug combinations were delivered in a total volume of 0.25 μl at a rate of 1 μl•min^{-1} by a 33 gauge stainless steel injector needle that extended 2 mm beyond the end of the guide cannula. The injector was left in place for an additional 45 s to allow drug to diffuse properly into the target region. Each rat received only one dose of drug and was used once. At the conclusion of behavioral testing, the rat was euthanized by overdose with CO_2 and the brain was removed and fixed by immersion in 4% formaldehyde-30% sucrose. Coronal sections through the pons were obtained with a cryostat microtome and stained with Cresyl violet. The microinjection site was identified by two persons blinded to the behavioral findings.

2.4. Experimental Design for Behavioral Studies

Experiments were conducted between 6 AM and 1 PM. The investigator was blinded to the identity of the drugs, although she could not be blinded to the treatment status of the rats due to inflammation of the hindpaw.

The first set of experiments examined the ability of DAMGO to increase PWL after microinjection in the right LC of saline- and CFA-treated rats. Baseline measures of weight, hindpaw thickness in the dorsoventral axis, and PWL were made. The rats were then prepared with an intracerebral guide cannula as described above and while still anesthetized received an intraplantar injection of 50 μl CFA (50 μg *Mycobacterium butyricum*, 85% Marcol 52, and 15% Aracel A mannide monoemulsifier; Calbiochem, LaJolla, CA) or 0.9% saline (pH 7.4) in the left hindpaw. Rats in each litter were randomly allocated to either CFA or saline treatment. Four days later, body weight, hindpaw thickness and PWL were redetermined. The rat was then gently restrained in a towel for microinjection of saline (pH 7.4) or DAMGO (0.3 – 3 ng) into the LC. Paw withdrawal latencies were recorded for each hindpaw 15, 30, and 60 min after microinjection. Quantitative assessments of sedation or catatonia were not made. However, gross observations of changes in behavior (catatonia, agitation, ataxia, sedation), as well as levels of alertness and orientation to a cotton applicator were recorded throughout the period of testing.

The second set of experiments determined whether microinjection of CTAP, a MOPr antagonist, in the right LC of saline- and CFA-treated rats decreased PWL. The design was as for the first set of experiments, except that 33 ng CTAP was microinjected in the LC. As these experiments were conducted concurrently with the first set, it was not necessary to generate a second set of saline controls. These experiments were preceded by an ancillary experiment in which 33 ng of CTAP was coadministered with 1 ng DAMGO in the LC of saline- and CFA-treated rats to verify that this dose could antagonize the antinociceptive and anti-hyperalgesic effects of the MOPr agonist.

Data were reported as mean ± S.E.M. The effects of CFA on paw thickness, PWL and weight were compared to that of saline by a two-way repeated measures ANOVA in which one factor was time (before and after injection) and the other factor was treatment (CFA or saline). Posthoc comparisons among individual group means were made by Bonferroni's test. The effects of DAMGO on PWL as a function of time were compared to that of saline by a two-way repeated measure ANOVA in which dose was one factor and time was the repeated factor. Posthoc comparisons among individual group means were made with Newman-Keuls' test. Two approaches were used to generate dose response curves for DAMGO. The first approach fit the data obtained at the time of maximal effect (15 min) to a least squares linear regression. The second approach incorporated both peak effect and duration of effect by calculating the area under the time-effect curve from 0 through 30 min, and using these data to generate a dose-response relationship. For this analysis, the baseline value was the PWL measured immediately before microinjection of drug. A $p < 0.05$ was considered significant.

2.5. Receptor Binding Assay

Rats were briefly anesthetized with halothane at 24 days of age, and an intraplantar injection of 50 μl CFA or pH 7.4 saline was made in the left hindpaw. Rats within a litter were randomly allocated to receive CFA or saline. Four days later, the rats were decapitated, the whole brain was transferred into ice-cold water and the cerebellum was dissected away. A 1–2 mm thick transverse section of brainstem that extended from the level of cranial nerve tract VII to the level of the inferior colliculus was removed and rapidly cooled on dry ice. A disposable biopsy punch (Electron Microscopy Services, Hatfield, PA) was then used to remove a crescent area on each side that contained the LC, the subcoeruleus and, because the dendrites of LC neurons

extend for several hundred microns (Shipley et al., 1996), the pericoerulear area as well. Although the diameter of the punch tool was 2 mm, the tissue taken was not 2 mm in diameter as a substantial part of the tool was positioned over the ventricle (Fig. 1). After removal of the LC, the tissue section was sliced and stained with Cresyl violet to verify that the LC from each side had been removed.

It was necessary to pool tissue punches from 10 CFA-treated rats and 10 saline-treated rats (representing two litters) to obtain sufficient amounts of membrane for a single binding experiment. The LC from both sides of each animal were pooled to maximize tissue and because unilateral inflammatory injury causes bilateral activation of LC neurons (Tsuruoka et al., 2003). Bilateral LC punches from 10 rats yielded 80–100 mg tissue before homogenization. Tissue was homogenized in 20 volumes (w/v) of ice-cold membrane buffer (50 mM TRIZMA, pH 7.4) using a Potter-Elvenjhem glass homogenizer and Teflon pestle. Homogenates were centrifuged at 39,400 g at 4°C for 15 min and the pellet was resuspended in homogenization buffer. After incubation for 10 min at 25°C to allow for the degradation of endogenous ligands, homogenates were again centrifuged at 39,400 g at 4°C for 15 min and the pellet resuspended in homogenization buffer. Homogenates were then frozen at −70°C. Protein concentration was determined using bovine serum albumin as a standard (Lowry et al., 1951). Membrane homogenates were coded to blind the investigator to the treatment condition.

Preliminary studies were conducted to optimize the experimental design. Linearity of binding was confirmed between 20 and 186 μg protein/tube, and it was determined that 100 μg protein/tube was sufficient. The saturation binding assay was conducted in triplicate. Membrane preparations from saline- and CFA-treated rats were processed concurrently in each experiment. Membranes (100–129 μg/tube) were incubated at 25°C in eight concentrations of [D-Ala^2, N-Methyl-Phe^4, Glyol^5] [tyrosyl-3,5-3H]enkephalin (specific activity 65 Ci/mmol; Amersham Biosciences; Piscataway, NJ) for 1 h in the presence and absence of 10 μM naloxone hydrochloride (RBI; Natick, MA). Total assay volume was 500 μl/tube. The reaction was terminated by rapid vacuum filtration over Whatman GF/B filters coated with 0.1% polyethyleneimine (2 h, 4°C) in a Brandel Cell Harvester, and three 5 ml washes with ice-cold buffer (50 mM TRIZMA, pH 7.2). Filter papers were washed with 500 μl absolute ethanol, equilibrated overnight at 25°C in scintillation counting fluid and counted in a liquid scintillation analyzer (Beckman LS 6500).

Specific binding was calculated as the difference of nonspecific binding from total binding. Counts per minute were converted to femtomoles per milligram of protein. Saturation binding curves were fit by nonlinear regression and an F-test was conducted to determine whether the data were best fit by a one- or two-site model. The K_d and B_{max} values were determined using GraphPad Prism software (version 4.0, San Diego, CA). The K_d and B_{max} values were expressed as the mean ± S.E.M. of four independent experiments, each containing sets of tissue from CFA- and saline-treated rats. Student's t-test was used to compare values in saline- and CFA-treated rats. A $p < 0.05$ was considered significant.

2.6 Receptor Autoradiography

Rats were received an injection of CFA or saline as described above. Four days later, the rats were decapitated and the brainstem rapidly frozen in 2-methyl butane. A cryostat was used to cut serial sets of coronal sections of 10-μm thickness through the rostral caudal extent of the LC at −20°C. Each set was comprised of two serial sections, each thaw-mounted onto a different GoldPlus slide, allowed to air dry and stored with dessicant at −80°C. Tissue was rinsed several times in 50 mM Tris buffer, pH 7.4, containing 100 mM NaCl and then transferred to buffer containing 7.5 [^{3}H]DAMGO (NIDA; 48 Ci/mmol) to determine total binding. The adjacent sections were transferred to buffer containing the radioligand and 100 nM unlabeled naloxone to determine non-specific binding. After sixty minutes, the sections

were rinsed several times with 50 mM Tris buffer, pH 7.4, containing $MgCl_2$. The sections were air-dried and, along with [^{3}H] microscales, apposed to a Fujifilm imaging plate for eight weeks. Images were obtained with a BAS 5000 phosphorimager and densitometric measurements were converted to fmol [^{3}H]DAMGO bound/mg tissue equivalent. Specific binding was determined by subtraction of non-specific binding from total binding. Values are reported as the mean and S.E.M. of determinations from three to six sections per animal; the left and right LC were averaged separately.

3. Results

3.1 Characteristics of the Model

Paw withdrawal latencies and hindpaw thicknesses of the 34 saline- and 35 CFA-treated rats used in this study are illustrated in Figure 2. Baseline PWLs for the ipsilateral and contralateral hindpaws did not differ within or between treatment groups ($p > 0.4$ for all comparisons). Four days after injection of CFA or saline, response latencies for the ipsilateral (left) hindpaw of CFA-treated rats were significantly shorter than for saline-treated rats ($p < 0.001$; Fig. 2A). Paw withdrawal latencies for the contralateral (right) hindpaw of CFA-treated rats (9.7 ± 0.2 s) were slightly longer than the corresponding hindpaw of saline-treated rats (9.1 ± 0.2 s), which may reflect a reluctance to shift weight to the inflamed hindpaw. While statistically significant due to the large N, the 0.6 s difference was not considered biologically significant as the mean value was well within the range of PWL recorded in naïve rats. The baseline thickness of the hindpaws did not differ within or between treatment groups ($p > 0.3$ for all comparisons; data not shown). However, four days after injection of CFA or saline, the ipsilateral hindpaw of CFA-treated rats was significantly larger than the corresponding paw of saline-treated rats ($p < 0.001$; Fig. 2B). Contralateral hindpaw thickness did not differ between the treatment groups ($p = 0.09$). These data confirm that injection of CFA in young rats produced thermal hyperalgesia and hindpaw inflammation as observed for adult rats (Hurley and Hammond, 2000;Sykes et al., 2007).

The average weight of pups before surgery was 54 ± 1 g for the saline-treatment group, and 56 ± 1 g for the CFA-treatment group. Average weight in the saline-treatment group was 69 ± 1 g at the completion of the study. Pups in the CFA-treatment group also weighed 69 ± 1 g. Thus, CFA-treated rats gained weight at the same rate as their saline-treated littermates, demonstrating that the persistent pain state did not interfere with feeding.

3.2. Antinociceptive Effects of DAMGO in Saline-treated Rats

In saline-treated rats, microinjection of 0.3 – 3 ng of DAMGO in the right LC or subcoeruleus produced a dose- and time-dependent increase in PWL of both ipsilateral (left) and contralateral (right) hindpaws (Fig. 3). Microinjection of saline in the LC of these rats did not alter PWL in either hindpaw. A representative microinjection site is illustrated in Fig. 1. Paw withdrawal latency was significantly increased after microinjection of 1 or 3 ng DAMGO into the LC (Fig. 3A, B). Microinjection of 0.3 ng DAMGO increased PWL only in the contralateral hindpaw. The increase in PWL was maximal within 15 min of microinjection, diminished at 30 min, and was essentially absent by 60 min. Although DAMGO was microinjected in the right LC, PWL was increased to an equivalent extent in both ipsilateral and contralateral hindpaws. This result was expected based on prior reports that LC neurons project bilaterally to the dorsal horn in Harlan Sprague-Dawley rats (Howorth et al., 2009;Proudfit and Clark, 1991), and that electrical stimulation of the LC increases PWL in both hindpaws to the same extent (West et al., 1993 1049). Microinjection of doses ≤ 3 ng in the LC or subcoeruleus did not produce sedation or ataxia, and the rats remained alert and able to orient to a cotton applicator. However, pilot studies with 10 ng DAMGO indicated that this dose produced frank sedation. Thus, doses > 3 ng were not tested.

Microinjection of 1 or 3 ng of DAMGO lateral to the LC in the medial parabrachial nucleus or superior cerebellar peduncle was substantially less effective (ipsilateral PWL: 11.8 ± 1.2 s; contralateral PWL: 12.5 ± 1.3 s; N=9). Similarly, microinjection of these doses at sites medial to the LC in the posterodorsal tegemental nucleus was also less effective (ipsilateral PWL: 12.3 ± 2 s; contralateral PWL: 10.5 ± 0.3 s; N = 4). However, microinjection of 1 or 3 ng DAMGO in the lateral parabrachial nucleus at the most rostral pole of the LC did increase PWL (ipsilateral: 14.6 ± 1.7, contralateral: 14.3 ± 1.3 s; N=6).

3.3. Antinociceptive and Anti-hyperalgesic Effects of DAMGO in CFA-treated Rats

In CFA-treated rats, microinjection of 0.3 – 3 ng of DAMGO in the LC also produced a dose- and time-dependent increase in PWL of both ipsilateral and contralateral hindpaws (Fig. 3C,D). Microinjection of saline produced a slight increase in PWL in ipsilateral hindpaws of the CFA-treated rats that was evident at both 15 and 30 min. Microinjection of 0.3 ng DAMGO slightly increased PWL in the ipsilateral and contralateral hindpaw compared to baseline values. However, these increases did not differ from those produced by saline. Microinjection of 1 or 3 ng DAMGO into the LC completely reversed hyperalgesia in the ipsilateral hindpaw. These doses also increased PWL in the contralateral hindpaw. As in saline-treated rats, peak effects for all doses occurred within 15 min of microinjection. However, the increase in PWL in the contralateral hindpaw of CFA-treated rats was less than that observed in saline-treated rats (compare Fig. 3B and 3D; see below). Moreover, the duration of effect was greatly truncated and the effects were absent by 30 min.

3.4. Antinociceptive Effects of DAMGO are Reduced in CFA-treated Rats

Figure 4 illustrates the dose-effect relationships for DAMGO in both saline- and CFA-treated rats. For the ipsilateral hindpaw, the dose-response curve in CFA-treated rats was parallel to that in saline-treated rats and shifted to the right. Comparison of the effects of DAMGO for the ipsilateral hindpaws of CFA- and saline-treated rats was confounded by the 3 s difference in baseline PWLs. Furthermore, in CFA-treated rats, the effect of DAMGO is to reverse hyperalgesia, whereas in the saline-treated rats the effect is to produce antinociception. The present study design therefore does not enable any conclusions to be drawn about the impact of persistent inflammatory nociception on the anti-hyperalgesic effects of DAMGO. The data are illustrated for the sake of completeness.

Comparisons were not confounded for the contralateral hindpaw. Baseline PWL for the contralateral hindpaws of CFA- and respective saline-treated rats did not differ for any dose group ($p > 0.4$, all groups), and the effect of the drug in both treatment groups was to produce antinociception. For the contralateral hindpaw, the dose-response relationship for DAMGO in CFA-treated rats was shifted to the right and downward from that in saline-treated rats with a significant reduction observed at 1 and 3 ng DAMGO in CFA-treated rats.

A drawback of dose-response curves generated at time of peak effect is that they fail to integrate the duration of effect. The duration of the effect of DAMGO in CFA-treated rats was significantly shorter than that in saline-treated rats (Fig. 3). Therefore, to integrate the factors of duration and magnitude of effect, an area under the curve (AUC) analysis was conducted. The AUC values for the increase in PWL of the contralateral hindpaw after microinjection of saline, 0.3, 1 or 3 ng DAMGO into the LC of saline-treated rats were 294 ± 17.2, 331.2 ± 22.95, 401 ± 26.1 and 378 ± 16.7, respectively. The AUC values for the increase in PWL of the contralateral hindpaw produced by these same doses in CFA-treated rats were 313.6 ± 14.4, 307.6 ± 8.0, 343.9 ± 10.2, and 327.9 ± 16.25. The antinociceptive effects of both 1 and 3 ng DAMGO were greatly reduced in the contralateral hindpaw of CFA-treated rats compared to saline-treated rats ($p < 0.05$). Furthermore, while 1 and 3 ng doses of DAMGO produced a significant antinociceptive effect in the contralateral hindpaw of saline-treated rats at 15 min,

none of the doses differed from the effect of saline in CFA-treated rats ($p > 0.1$) when measuring AUC. As stated previously, comparisons of the effects of DAMGO for the ipsilateral hindpaws of CFA- and saline-treated rats were confounded due to differences in the baseline PWL and the AUC values are therefore not presented.

Diffusion of drug into the cerebrospinal fluid with a consequent action at remote sites is a concern when targeting sites that lie adjacent to the ventricles. To examine whether this was factor, the effects of DAMGO microinjected in the ventricle of saline- and CFA-treated rats were compared. The time-course of the effect was identical to that observed after microinjection in the LC, with maximal increases in PWL evident 15 min after microinjection. Microinjection of 1 ng DAMGO in the ventricles of four saline-treated rats increased contralateral PWL to 11.9 ± 1.1 s, whereas this same dose increased contralateral PWL to 14.3 ± 1.5 s in six CFA-treated rats. Thus, this dose of DAMGO was less effective when injected into the ventricles of saline-treated rats as compared to the LC (See Fig. 2B). Also, when injected into the ventricles of CFA-treated rats, the effect was unchanged and even marginally enhanced, rather than diminished as observed after injection in the LC. These observations complement the placement controls in adjacent parenchyma and indicate that the site of drug action is in the LC.

3.5. Microinjection of CTAP Does Not Alter PWL in Saline or CFA-treated Rats

Figure 5 (upper panel) demonstrates that coadministration of 33 ng CTAP significantly antagonized the antinociceptive effects of 1 ng DAMGO microinjected in the LC of in rats treated four days earlier with saline. These data establish the efficacy of this dose and are consistent with a previous report that 15 min is an optimal treatment time for CTAP (Hurley and Hammond, 2000). When microinjected in the LC of saline-treated rats, this dose of CTAP alone did not decrease PWL of either hindpaw compared to the effects of saline or compared to baseline latencies. When microinjected in the LC of CFA-treated rats (Fig. 5, lower panels), this dose of CTAP also did not exacerbate the hyperalgesia in the ipsilateral hindpaw or induce hyperalgesia in the contralateral hindpaw compared to the effects of saline or to baseline response latencies. The antagonism of the anti-hyperalgesic effect of 1 ng DAMGO in the ipsilateral hindpaw of CFA-treated rats by CTAP did not achieve statistical significance ($p = 0.06$; two-tailed t-test).

3.6. CFA Treatment Reduces the B_{max}, but Not the K_d of MOPr in the LC

Four replicates of the saturation binding experiment were conducted using tissue homogenates obtained from saline- and CFA-treated rats. Figure 1 illustrates how the punch was used to obtain the core LC, subcoeruleus and pericoerulear areas. Figure 6 illustrates representative saturation isotherms from a single experiment with both treatment groups. Saturation isotherms in both treatment groups were tested for their fit to a one- or two-site model. The one-site model was consistently preferred in all four data sets for the CFA treatment group. Although the two-site model produced a statistically better fit in three of the four data sets in the saline-treatment group, it also yielded K_d and B_{max} values that were out of the range of the experimental concentrations of [^{3}H]DAMGO. This may be attributed to an insufficient number of doses at lower concentrations of radioligand. All four data sets for the saline-treatment group fit the one-site model with r^2 values exceeding 0.87. The one-site model also yielded B_{max} and K_d values that agreed with estimates in the literature: B_{max} of 53.3 ±7.0 fmol/mg protein and 98.3 ±15.2 fmol/mg protein for caudal and rostral LC in 21-day old rats and K_d of 1.5 ± 0.1 nM in pons/medulla of adult rat (Xia and Haddad, 1991;Yeadon and Kitchen, 1988). Therefore, the one-site model was used to analyze and compare the data from both treatment groups. Mean values for K_d in the LC were 1.59 ± 0.22 nM in saline-treated rats and 1.0 ± 0.4 nM in CFA-treated rats. These values did not differ from each other ($p > 0.2$). However, the B_{max} value

for [^{3}H]DAMGO in the LC from CFA-treated rats was decreased by 50% (50.5 ± 5.2 fmol/mg protein in saline-treated rats vs 23.4 ± 4.2 fmol/mg protein in CFA-treated rats; $p < 0.01$).

The autoradiographic analysis confirmed a loss in the number binding sites for [^{3}H]DAMGO in CFA-treated rats and further demonstrated that the reduction in MOPr occurred bilaterally after a unilateral injury. In saline-treated rats (N=4), the amount bound to the left and right LC by a saturating concentration of DAMGO was 359.4 ± 20.9 and 327.5 ± 22.8 fmol/mg tissue equivalent, respectively. In CFA-treated rats (N=4), the amount bound was significantly reduced to 242.4 ± 13.5 and 221.3 ± 35.0 fmol/mg tissue equivalent in the left and right LC (each $p < 0.01$, respectively). These reductions correspond to 32.6% and 32.4% for the left and right sides, respectively. Figure 7 presents representative autoradiograms from a saline- and a CFA-treated rat.

4. Discussion

4.1. Ramifications of Persistent Inflammatory Nociception for Opioid Action in the LC

This study is the first to directly probe the ramifications of persistent inflammatory nociception for the actions of MOPr agonists in the LC, a pontine nucleus that not only regulates nociception, but also plays a key role in coordinating affective, autonomic and sensory responses to stress (Berridge and Waterhouse, 2003; Valentino and Van Bockstaele, 2005). It determined that the antinociceptive effects of the MOPr agonist DAMGO in male rats are significantly reduced in the LC under conditions of inflammatory nociception, most likely due to the concomitant decrease in the number of MOPr that occurs in the LC. These findings are in striking contrast to the RVM where the actions of *mu*, *delta* or *kappa* opioid receptor agonists are enhanced (Hurley and Hammond, 2000; Schepers et al., 2007), and in which the enhancement is not mediated by changes in receptor number or affinity (Sykes et al., 2007). The enhanced antinociceptive effect of MOPr agonists in the RVM is thought to represent a compensatory response by the organism to mitigate the full magnitude of thermal hyperalgesia or mechanical allodynia (Hurley and Hammond, 2000). The teleological basis for a reduction in the antinociceptive effects of a MOPr agonist in the LC is less clear, but several possibilities merit consideration. A loss of opioid-mediated inhibition in the LC will alter the balance of excitatory and inhibitory inputs to LC neurons and could function to preserve the saliency of the inflammatory pain state by enhancing the discharge rates of cortically- and thalamically-projecting LC neurons that mediate arousal and attention. It may also be a mechanism by which the responses of LC neurons to different, heterotypic stressors are enhanced or sensitized during periods of persistent pain. It may be a mechanism by which sleep patterns are altered in the face of unremitting painful stimuli. These effects may be important for an animal's ability to respond appropriately to non-noxious and noxious stimuli that are encountered after injury (Berridge and Waterhouse, 2003).

Three mechanisms may underlie the anti-hyperalgesic and antinociceptive effects of DAMGO in the LC. First, DAMGO may act postsynaptically to hyperpolarize and directly inhibit LC neurons (Williams and North, 1984) that project to the thalamus, where release of norepinephrine activates α_1 noradrenergic receptors and facilitates nociception (reviewed by Pertovaara, 2006). Second, MOPr agonists may act presynaptically to inhibit tonically-active GABAergic inputs to LC neurons that project to the spinal cord (Pan et al., 2004), where release of norepinephrine produces antinociception by activation of α_2 noradrenergic receptors (reviewed by Pertovaara, 2006). Third, MOPr agonists may act presynaptically to inhibit glutamatergic inputs to LC neurons that project rostrally, although not to those that project to the spinal cord (Pan et al., 2004). Release of glutamate in the LC is thought to mediate the activation of LC neurons by sensory stimuli (Valentino and Van Bockstaele, 2005). Whether the decrease in MOPr in CFA-treated rats involves presynaptic or postsynaptic receptors remains to be determined.

4.2. Potential Mechanisms for MOPr Downregulation in CFA-treated Rats

Neurons in the LC receive synaptic contacts from fibers that are immunoreactive for enkephalin (Van Bockstaele et al., 1995) and, to a lesser extent, endomorphin (Peoples et al., 2002). The LC and pericoerulear region also contain β-endorphin (Finley et al., 1981; Palkovits and Eskay, 1987) and an anterograde labeling study has identified an afferent input from neurons in the arcuate nucleus, a source of β-endorphin (Sim and Joseph, 1991). Sustained exposure to exogenous MOPr-selective agonists, particularly those of high efficacy or intrinsic activity, can induce a downregulation of MOPr (Yoburn et al., 2004). It was therefore posited that the decrease in MOPr in the LC of CFA-treated rats was the result of an enhanced or sustained release of endogenous opioid peptides that act at MOPr in the LC, and that persistent inflammatory nociception induced a state of endogenous tolerance. A similar proposal was recently made to explain the desensitization of MOPr and development of opioid tolerance in the striatum of mice with neuropathic pain (Petraschka et al., 2007). Analogous to the naloxone-precipitated withdrawal in morphine-tolerant rats, microinjection of CTAP in the LC was expected to exacerbate hyperalgesia in the ipsilateral, inflamed hindpaw, and possibly induce hyperalgesia in the contralateral, uninflamed hindpaw of CFA-treated rats. However, this did not occur in either saline-treated or CFA-treated rats. These data suggest that under normal conditions there is little or no tonic release of endogenous opioids that act at MOPr in the LC. The lack of effect of CTAP in CFA-treated rats does not support the hypothesis that the downregulation of MOPr in the LC of CFA-treated rats is the result of a sustained or increased release of endogenous MOPr-activating agonists. This finding contrasts with the ability of a *delta*, but not a MOPr antagonist to exacerbate thermal hyperalgesia in the ipsilateral hindpaw and induce hyperalgesia in the contralateral hindpaw when microinjected in the RVM of CFA-treated rats (Hurley and Hammond, 2000). It is possible that the release of endogenous opioids has returned to basal levels by 4 days, whereas the downregulation of MOPr persists. Unfortunately, this idea cannot be tested by continuous administration of CTAP because MOPr are upregulated after chronic administration of MOPr antagonists (Rajashekara et al., 2003; Sirohi et al., 2007). Nonetheless, the inability of CTAP to produce or exacerbate hyperalgesia in CFA-treated rats indicates that persistent inflammatory nociception does not induce a state of endogenous opioid tolerance in the LC. Another mechanism by which downregulation of MOPr may occur involves changes in the phosphorylation state of MOPr. The MOPr has 20 phosphorylation sites on various Ser, Thr and Tyr residues that differentially regulate receptor uncoupling and internalization (reviewed by Celver et al., 2004; Connor et al., 2004; Law et al., 2000). Changes in the phosphorylation state of MOPr in CFA-treated rats could result in enhanced MOPr internalization and an increased targeting of MOPr to degradative pathways.

4.3. Other Considerations

A modest anti-hyperalgesia was observed up to 30 min after microinjection of saline in the LC of CFA-treated rats. Microinjection involves a brief period (< 2 min) of restraint. The LC is activated during acute restraint (Medeiros et al., 2003), and activation of LC neurons can produce antinociception (reviewed by Pertovaara, 2006). Thus, the slight increase in PWL that occurred in the ipsilateral hindpaw of CFA-treated rats after microinjection of saline may be attributed to an increase in the activity of LC neurons due to the brief restraint. This supposition is supported by the fact that the increase in PWL did not occur when CTAP was microinjected in the LC.

In vitro electrophysiological studies of MOPr function in LC neurons in slices prepared from adult rats report that the LC has a large reserve of MOPr, and that significant downregulation or uncoupling (> 75%) must occur before decrements in the potency or efficacy of highly efficacious agonists are apparent (reviewed by Connor et al., 2004). In this study, the B_{max} of MOPr in the LC was decreased by 50% in CFA-treated rats and was accompanied by a decrease in the antinociceptive effect of DAMGO, a highly efficacious agonist. Although the number

of MOPr in the LC does not differ between 21-day old and adult rats (52.5 fmol/mg protein vs 42.4 fmol/mg protein for caudal LC) (Xia and Haddad, 1991), the receptor reserve or the efficiency of coupling to $G_{i/o}$ may not be as great in 4-week old rats as in adult rats (Talbot et al., 2005).

4.4. Summary

These results provide new evidence that persistent inflammatory nociception alters the antinociceptive actions of MOPr agonists in the CNS by diverse mechanisms that are specific to the nucleus and likely to have different teleological bases. In the LC of CFA-treated rats, the antinociceptive effects of DAMGO are decreased both in magnitude and in duration of effect. These results are most directly explained by the finding that MOPr is downregulated in the LC under conditions of persistent inflammatory nociception. This conclusion is further supported by the results of whole-cell voltage clamp recordings in which the efficacy of DAMGO to produce outward currents in LC neurons from CFA-treated rats is reduced by about 50% (Jongeling et al., 2005). Although a sustained release endogenous opioids that act at MOPr was hypothesized to be responsible for the reduction in MOPr expression, the experimental data do not strongly support the idea of endogenous opioid-mediated tolerance because the MOPr antagonist CTAP did not exacerbate or induce hyperalgesia in CFA-treated rats. Mechanisms of long-term downregulation of MOPr are not well understood. Possibilities worthy of further investigation include activation of receptor tyrosine kinases and G protein kinases that phosphorylate MOPr and direct the internalized receptor to degradative pathways, as well as events that regulate transcription.

Acknowledgements

We thank Stephanie White, Adam Simonsen and Julie Coyne for technical assistance. This work was supported by grants from the National Institute on Drug Abuse: R01 DA06736 to D.L.H., F30 DA019767 to A.C.J. and R01 DA 016272 to A.Z.M.

References

Berridge CW, Waterhouse BD. The locus coeruleus-noradrenergic system: modulation of behavioral state and state-dependent cognitive processes. Brain Res Rev 2003;42:33–84. [PubMed: 12668290]

Celver J, Xu M, Jin W, Lowe J, Chavkin C. Distinct domains of the μ-opioid receptor control uncoupling and internalization. Mol Pharmacol 2004;65:528–537. [PubMed: 14978231]

Clement CI, Keay KA, Owler BK, Bandler R. Common patterns of increased and decreased fos expression in midbrain and pons evoked by noxious deep somatic and noxious visceral manipulations in the rat. J Comp Neurol 1996;366:495–515. [PubMed: 8907361]

Connor M, Osborne PB, Christie MJ. Mu-opioid receptor desensitization: is morphine different? Br J Pharmacol 2004;143:685–696. [PubMed: 15504746]

Ding YQ, Kaneko T, Nomura S, Mizuno N. Immunohistochemical localization of μ-opioid receptors in the central nervous system of the rat. J Comp Neurol 1996;367:375–402. [PubMed: 8698899]

Finley JC, Lindstrom P, Petrusz P. Immunocytochemical localization of β-endorphin-containing neurons in the rat brain. Neuroendocrinology 1981;33:28–42. [PubMed: 6265819]

Hirata H, Aston-Jones G. A novel long-latency response of locus coeruleus neurons to noxious stimuli: mediation by peripheral C-fibers. J Neurophysiol 1994;71:1752–1761. [PubMed: 8064346]

Howorth PW, Teschemacher AG, Pickering AE. Retrograde adenoviral vector targeting of nociresponsive pontospinal noradrenergic neurons in the rat in vivo. J Comp Neurol 2009;512:141–157. [PubMed: 19003793]

Hurley RW, Hammond DL. The analgesic effects of supraspinal μ and δ opioid receptor agonists are potentiated during persistent inflammation. J Neurosci 2000;20:1249–1259. [PubMed: 10648729]

Hurley RW, Hammond DL. Contribution of endogenous enkephalins to the enhanced analgesic effects of supraspinal μ opioid receptor agonists after inflammatory injury. J Neurosci 2001;21:2536–2545. [PubMed: 11264327]

Jongeling, AC.; Zhang, L.; Hammond, DL. Effects of inflammatory pain on mu opioid responses in locus coeruleus (LC). Program No. 394.8 2005. Neuroscience Meeting Planner. Society for Neuroscience; Washington, DC. 2005.

Law PY, Wong YH, Loh HH. Molecular mechanisms and regulation of opioid receptor signaling. Annu Rev Pharmacol Toxicol 2000;40:389–430. [PubMed: 10836142]

Lowry OH, Rosebrough NJ, Farr AL, Randall RJ. Protein measurement with the Folin phenol reagent. J Biol Chem 1951;193:265–275. [PubMed: 14907713]

Mansour A, Fox CA, Burke S, Meng F, Thompson RD, Akil H, Watson SJ. Mu, delta and kappa opioid receptor mRNA expression in the rat CNS: an in situ hybridization study. J Comp Neurol 1994;350:412–438. [PubMed: 7884049]

Medeiros MA, Canteras NS, Suchecki D, Mello LE. c-Fos expression induced by electroacupuncture at the Zusanli point in rats submitted to repeated immobilization. Braz J Med Biol Res 2003;36:1673–1684. [PubMed: 14666252]

Millan MJ. Descending control of pain. Prog Neurobiol 2002;66:355–474. [PubMed: 12034378]

Palkovits M, Eskay RL. Distribution and possible origin of β-endorphin and ACTH in discrete brainstem nuclei of rats. Neuropeptides 1987;9:123–137. [PubMed: 3033542]

Pan YZ, Li DP, Chen SR, Pan HL. Activation of μ-opioid receptors excites a population of locus coeruleus-spinal neurons through presynaptic disinhibition. Brain Res 2004;997:67–78. [PubMed: 14715151]

Peoples JF, Wessendorf MW, Pierce T, Van Bockstaele EJ. Ultrastructure of endomorphin-1 immunoreactivity in the rat dorsal pontine tegmentum: evidence for preferential targeting of peptidergic neurons in Barrington's nucleus rather than catecholaminergic neurons in the peri-locus coeruleus. J Comp Neurol 2002;448:268–279. [PubMed: 12115708]

Pertovaara A. Noradrenergic pain modulation. Prog Neurobiol 2006;80:53–83. [PubMed: 17030082]

Petraschka M, Li S, Gilbert TL, Westenbroek RE, Bruchas MR, Schreiber S, Lowe J, Low MJ, Pintar JE, Chavkin C. The absence of endogenous β-endorphin selectively blocks phosphorylation and desensitization of mu opioid receptors following partial sciatic nerve ligation. Neuroscience 2007;146:1795–1807. [PubMed: 17467916]

Porro CA, Tassinari G, Facchinetti F, Panerai AE, Carli G. Central beta-endorphin system involvement in the reaction to acute tonic pain. Exp Brain Res 1991;83:549–554. [PubMed: 2026197]

Proudfit HK, Clark FM. The projections of locus coeruleus neurons to the spinal cord. Prog Brain Res 1991;88:123–141. [PubMed: 1813919]

Rajashekara V, Patel CN, Patel K, Purohit V, Yoburn BC. Chronic opioid antagonist treatment dose-dependently regulates μ-opioid receptors and trafficking proteins in vivo. Pharmacol Biochem Behav 2003;75:909–913. [PubMed: 12957235]

Schepers RJ, Mahoney JL, Shippenberg TS. Inflammation-induced changes in rostral ventromedial medulla μ and κ opioid receptor mediated antinociception. Pain. 200710.1016/j.pain.2007.07.010

Shipley MT, Fu L, Ennis M, Liu WL, Aston-Jones G. Dendrites of locus coeruleus neurons extend preferentially into two pericoerulear zones. J Comp Neurol 1996;365:56–68. [PubMed: 8821441]

Sim LJ, Joseph SA. Arcuate nucleus projections to brainstem regions which modulate nociception. J Chem Neuroanat 1991;4:97–109. [PubMed: 1711859]

Sirohi S, Kumar P, Yoburn BC. μ-opioid receptor up-regulation and functional supersensitivity are independent of antagonist efficacy. J Pharmacol Exp Ther 2007;323:701–707. [PubMed: 17698975]

Sykes KT, White SR, Hurley RW, Mizoguchi H, Tseng LF, Hammond DL. Mechanisms responsible for the enhanced antinociceptive effects of μ-opioid receptor agonists in the rostral ventromedial medulla of male rats with persistent inflammatory pain. J Pharmacol Exp Ther 2007;322:813–821. [PubMed: 17494863]

Talbot JN, Happe HK, Murrin LC. μ opioid receptor coupling to $G_{i/o}$ proteins increases during postnatal development in rat brain. J Pharmacol Exp Ther 2005;314:596–602. [PubMed: 15860573]

Tsuruoka M, Arai YC, Nomura H, Matsutani K, Willis WD. Unilateral hindpaw inflammation induces bilateral activation of the locus coeruleus and the nucleus subcoeruleus in the rat. Brain Res Bull 2003;61:117–123. [PubMed: 12831996]

Tsuruoka M, Hitoto T, Hiruma Y, Matsui Y. Neurochemical evidence for inflammation-induced activation of the coeruleospinal modulation system in the rat. Brain Res 1999;821:236–240. [PubMed: 10064809]

Tsuruoka M, Willis WD. Descending modulation from the region of the locus coeruleus on nociceptive sensitivity in a rat model of inflammatory hyperalgesia. Brain Res 1996;743:86–92. [PubMed: 9017234]

Valentino, RJ.; Van Bockstaele, EJ. Functional interactions between stress neuromediators and the locus coeruleus-noradrenaline system. In: Steckler, T.; Kalin, NH.; Reul, JMHM., editors. Handbook of Stress and the Brain. Elsevier; Amsterdam: 2005. p. 465-486.

Van Bockstaele EJ, Branchereau P, Pickel VM. Morphologically heterogeneous met-enkephalin terminals form synapses with tyrosine hydroxylase-containing dendrites in the rat nucleus locus coeruleus. J Comp Neurol 1995;363:423–438. [PubMed: 8847409]

Wei F, Dubner RKR. Nucleus reticularis gigantocellularis and nucleus raphe magnus in the brain stem exert opposite effects on behavioral hyperalgesia and spinal Fos protein expression after peripheral inflammation. Pain 1999;80:127–141. [PubMed: 10204725]

West WL, Yeomans DC, Proudfit HK. The function of noradrenergic neurons in mediating antinociception induced by electrical stimulation of the locus coeruleus in two different sources of Sprague-Dawley rats. Brain Res 1993;626:127–135. [PubMed: 7904225]

Williams JT, North RA. Opiate-receptor interactions on single locus coeruleus neurones. Mol Pharmacol 1984;26:489–497. [PubMed: 6092898]

Xia Y, Haddad GG. Ontogeny and distribution of opioid receptors in the rat brainstem. Brain Res 1991;549:181–193. [PubMed: 1653081]

Yeadon M, Kitchen I. Comparative binding of μ and δ selective ligands in whole brain and pons/medulla homogenates from rat: affinity profiles of fentanyl derivatives. Neuropharmacology 1988;27:345–348. [PubMed: 2843777]

Yoburn BC, Purohit V, Patel K, Zhang Q. Opioid agonist and antagonist treatment differentially regulates immunoreactive μ-opioid receptors and dynamin-2 in vivo. Eur J Pharmacol 2004;498:87–96. [PubMed: 15363980]

Zangen A, Herzberg U, Vogel Z, Yadid G. Nociceptive stimulus induces release of endogenous β-endorphin in the rat brain. Neuroscience 1998;85:659–662. [PubMed: 9639262]

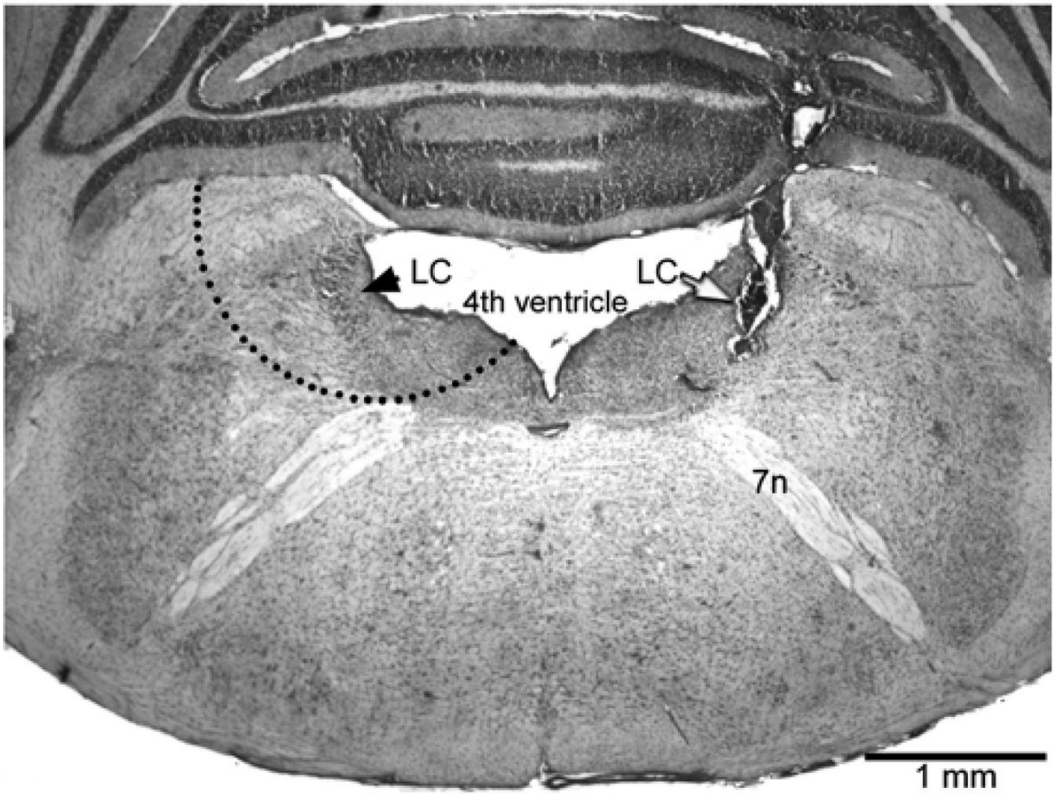

Fig. 1.

Photomicrograph of a representative microinjection site (white arrow) in the right locus coeruleus (LC). The coronal section is stained with Cresyl violet. The black arrow identifies the left LC. The dashed semi-circle illustrates how the punch tool was applied to obtain the core LC and pericoerulear areas; the cerebellum would have been removed prior to punching. 7n: 7th cranial nerve

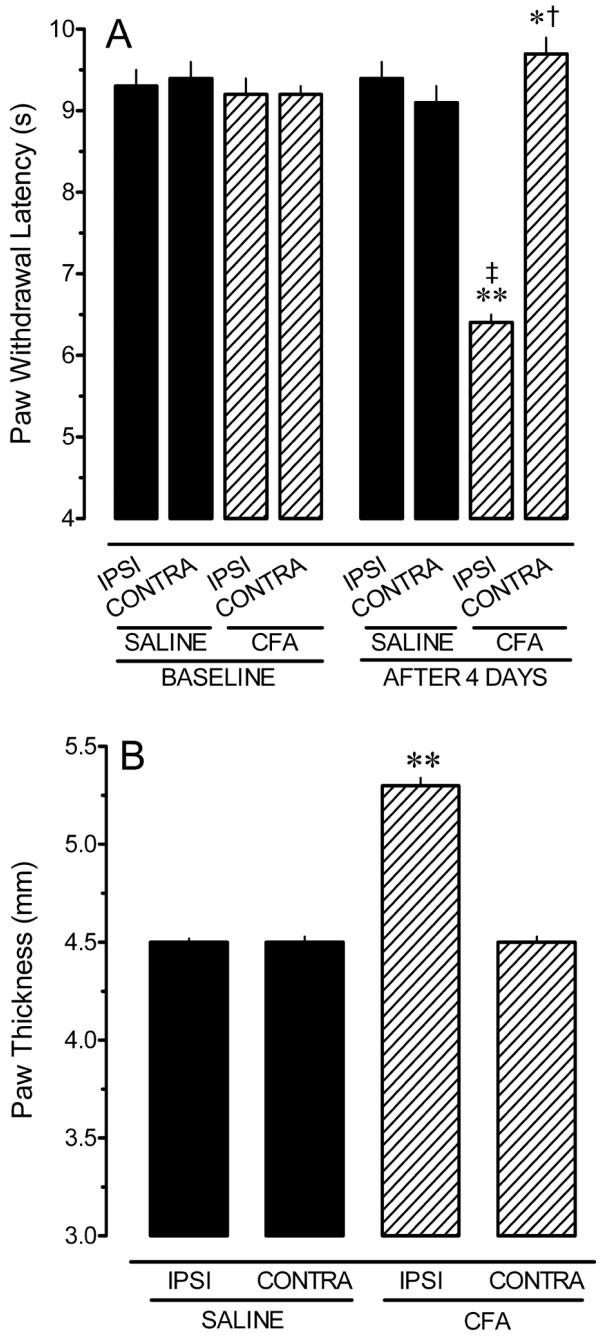

Fig. 2.

Intraplantar injection of complete Freund's adjuvant (CFA) induces thermal hyperalgesia (A) and inflammation (B) in the ipsilateral hindpaw four days later. Values represent the mean ± S.E.M. of determinations in 35 saline-treated and 34 CFA-treated rats. In panel B only data obtained 4 days after injection of CFA or saline are shown; error bars are too small to be seen. * $p < 0.05$, ** $p < 0.01$ compared to corresponding paw in saline-treated group. † $p < 0.05$, ‡ $p < 0.01$ compared to baseline within that treatment group.

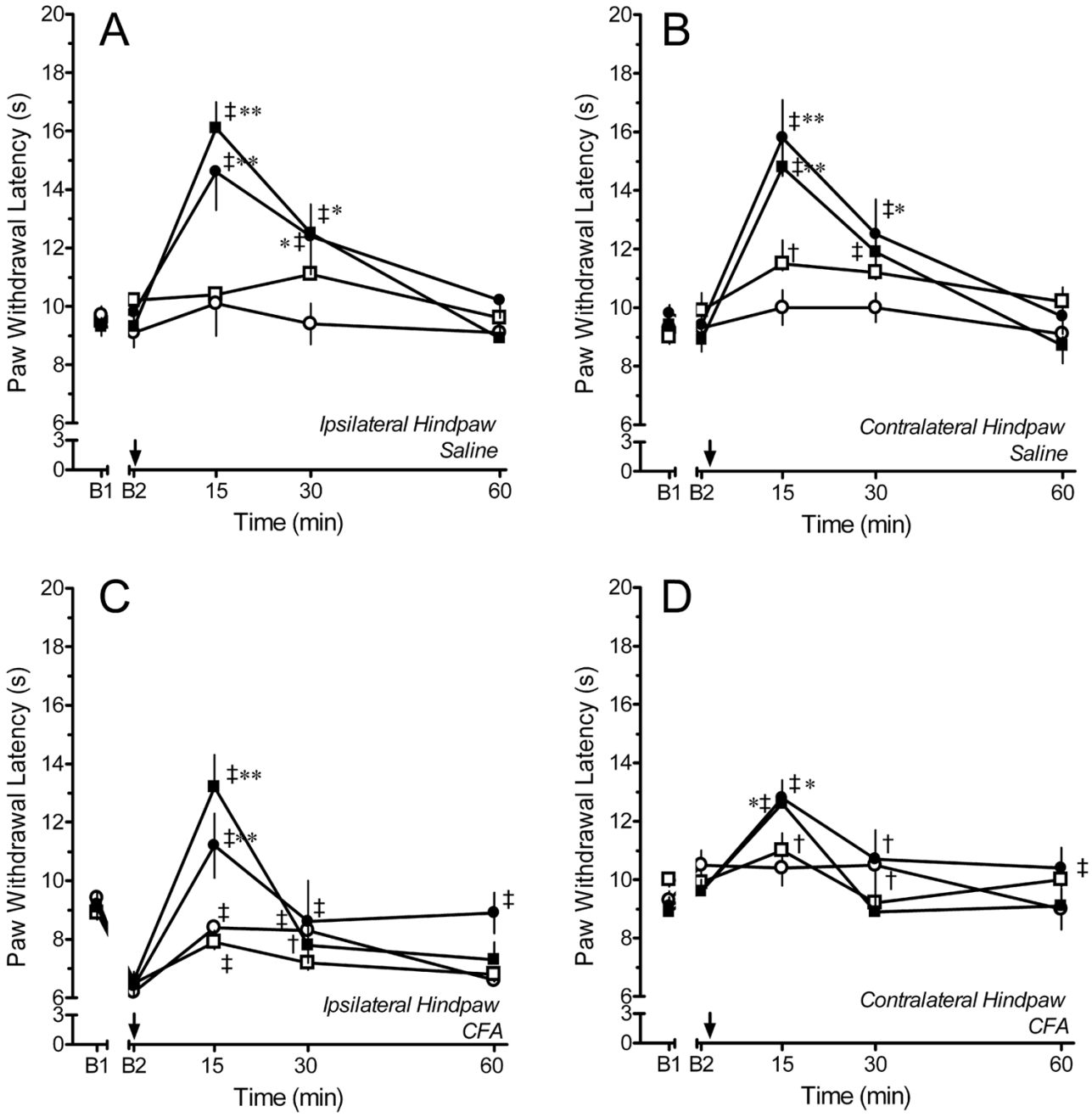

Fig. 3.

Time course of paw withdrawal latency (PWL) after microinjection of saline (open circles; N=4–7), 0.3 ng (open squares; N=3–4), 1 ng (filled circles; N=7 each), or 3 ng (filled squares; N=8–10) of DAMGO into the locus coeruleus (LC) of rats that had received an injection of saline (A, B) or CFA (C,D) in the left hindpaw four days earlier. Note that the increase in contralateral PWL produced by 1 and 3 ng DAMGO in CFA-treated rats is less than that observed in saline-treated rats. Comparisons of the ipsilateral PWL are confounded by differing baselines. B1 represents the baseline PWL determined before hindpaw injection of saline or CFA. B2 represents the baseline PWL determined 4 days later and before microinjection of

saline or DAMGO in the LC. Arrow denotes time of microinjection. † $p < 0.05$, ‡ $p < 0.01$ compared to B2; * $p < 0.05$, ** $p < 0.01$ compared to saline at the corresponding time point.

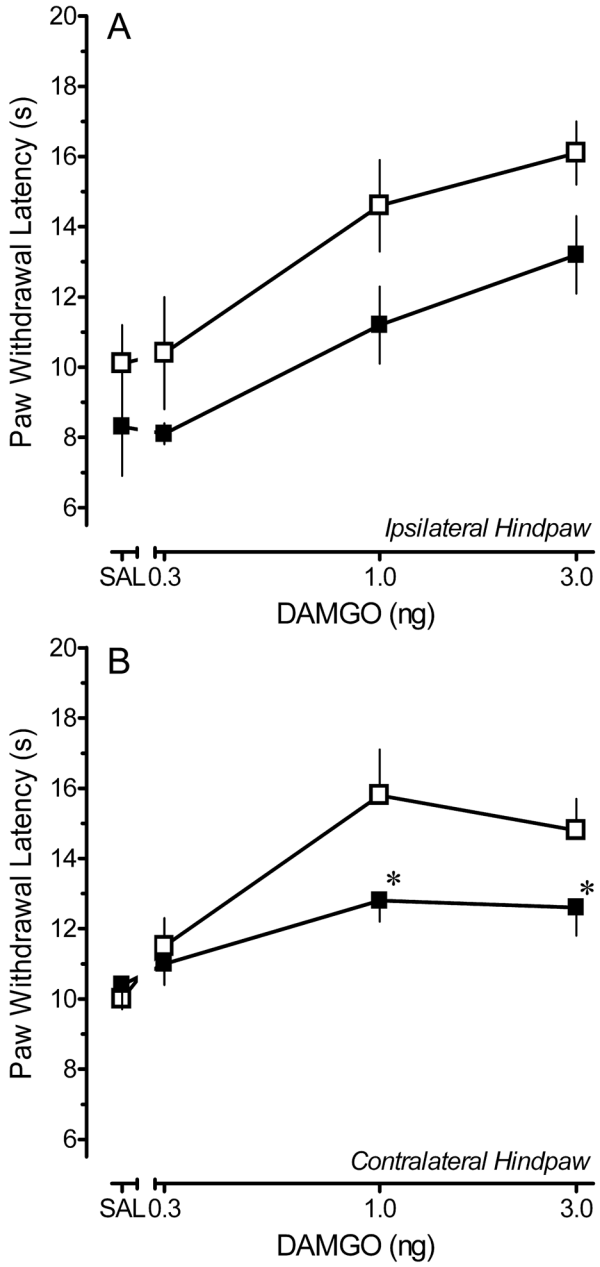

Fig. 4.

Dose response relationships for the peak increase in paw withdrawal latency (PWL) produced by microinjection of saline (SAL) or 0.3–3 ng DAMGO in the locus coeruleus of saline- or CFA-treated rats. Data were obtained at 15 min, the time of peak effect. (A) Ipsilateral hindpaw. (B) Contralateral hindpaw. Each symbol represents the mean ± S.E.M. of determinations in 3–10 rats. Open squares: saline-treated rats. Solid squares: CFA-treated rats. * $p < 0.05$ compared with corresponding dose in saline-treated group.

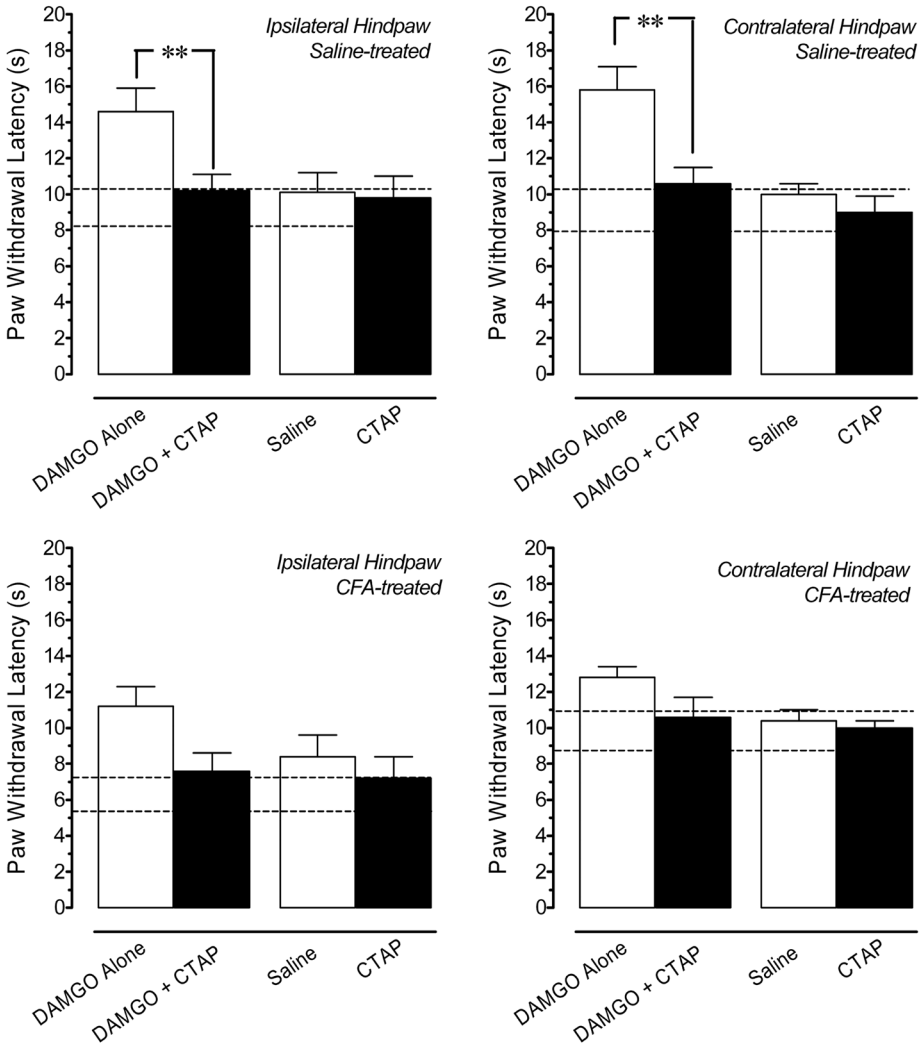

Fig. 5.

Effects of CTAP on paw withdrawal latency (PWL) in saline- and CFA-treated rats. Top panels: Coadministration of 33 ng CTAP antagonizes the antinociception produced by microinjection of 1 ng DAMGO in the locus coeruleus (LC) in saline-treated rats. Microinjection of this dose of CTAP alone in the LC does not alter PWL compared to the effects of saline alone. Bottom panels: In CFA-treated rats, microinjection of 33 ng CTAP alone into the LC does not exacerbate thermal hyperalgesia in the ipsilateral hindpaw, nor does it produce hyperalgesia in the contralateral hindpaw of CFA-treated rats compared to the effects of saline. The antagonism of the anti-hyperalgesic effect of 1 ng DAMGO in the ipsilateral hindpaw of CFA-treated rats by CTAP did not achieve statistical significance ($p = 0.06$; two-tailed t-test). Each bar is the mean ± S.E.M. of determinations in 4–7 rats. * $p < 0.05$, ** $p < 0.01$ compared to 1 ng DAMGO at the corresponding time point. Horizontal dashed lines delineate the upper and lower 1 SD from the mean baseline PWL determined for all rats immediately before microinjection of drug in the LC. Data are values determined 15 min after microinjection, the time of peak effect for all agents.

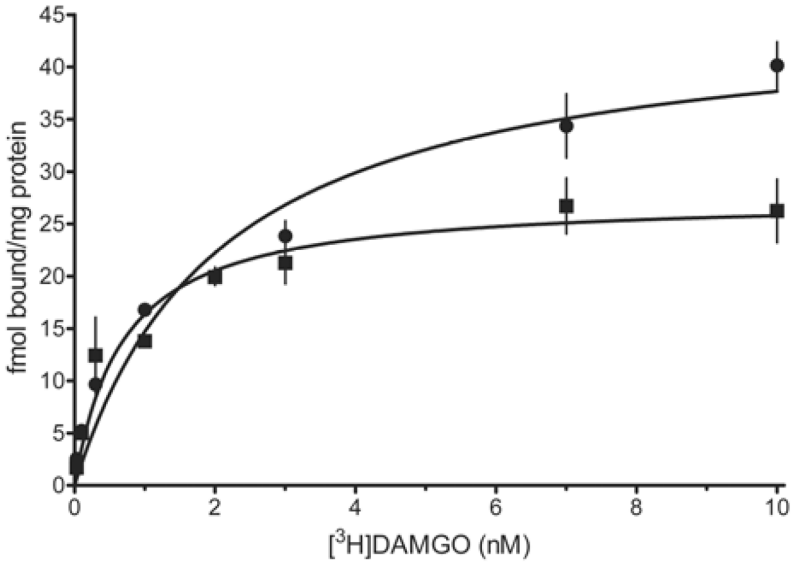

Fig. 6.

Representative saturation isotherms for specific binding of [^{3}H]DAMGO to membrane homogenates containing the locus coeruleus (LC) of 28-day old rats 4 days after intraplantar injection of complete Freund's adjuvant (squares) or saline (circles). Results illustrated are from a single experiment, in which tissue from 10 rats was pooled in each treatment group. Nonspecific binding was determined in the presence of 10 μM naloxone. Symbols are the mean ± S.E.M. of triplicate determinations.

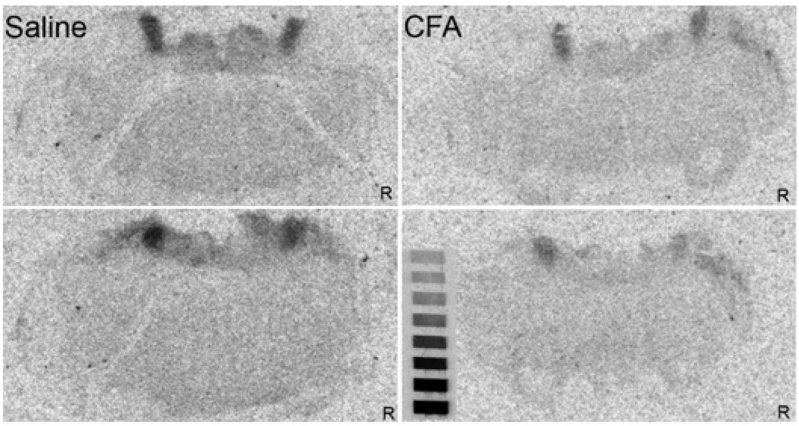

Fig. 7.

Autoradiograms for binding of a saturating concentration of [^{3}H]DAMGO (7.5 nM) to the locus coeruleus of a saline- or CFA-treated rat. Two different levels from the same animal are illustrated for each treatment condition. Note the uniform reduction in binding in both the right and the left LC of rats that received an injection of complete Freund's adjuvant in the left hindpaw. R indicates the right side of the brain. The microscale is included for reference. No adjustments to gain, brightness or contrast were made to these images.